Testing the response of cyanobacteria *Synechocystis* to PFOS using variable chlorophyll fluorescence and stable isotopes

Name: Veerle Troelstra
Student number: 6358098
Email: v.troelstra@uu.nl
Telephone: +31 0681256669
Date: March 2024

1st Supervisor: Dr. Lubos Polerecky
(Utrecht University)
l.polerecky@uu.nl

2nd Supervisor: Dr. Meri Eichner
(Czech Academy of Sciences)
eichner@alga.cz

Word count: 7017

1 Abstract

Polyfluoroalkyl substances (PFAS) constitute a widespread contaminant in the natural environment. Their resistance to degradation as a result of strong C–F bonds makes them largely unresponsive to conventional wastewater treatment methods. Bio-remediation, which uses organisms to break down contaminants, is an emerging approach that offers a cost-effective remediation technology with the potential for *in situ* treatment. In this study, we tested the potential of cyanobacteria *Synechocystis* for bio-remediation of perfluorooctanesulfonic acid (PFOS), which is one of the most common types of PFAS found in the environment. Our approach used (1) toxicology assays to determine the tolerance of *Synechocystis* to PFOS and (2) incubation experiments with ^{13}C-labelled PFOS to assess its bio-accumulation potential. The toxicology assays revealed that over a period of 7 days, which corresponds to 5 generations, growth rates were not significantly affected by PFOS up to the maximum tested concentration of 8 mg L^{-1}. The photosynthetic potential of *Synechocystis* across the exponential and stationary growth phases, measured by methods based on variable chlorophyll *a* fluorescence, was also unaffected within the tested range of PFOS concentrations. The bio-accumulation potential was tested at a PFOS concentration of 1 mg L^{-1}. In contrast to the expected increase in δ^{13}C as a result of ^{13}C-PFOS accumulation by the cells, we observed a small but significant decrease, indicative of no PFOS accumulation. Overall, this study demonstrates that the growth of *Synechocystis* on short time scales is not affected by PFOS until concentrations that by far exceed those found in surface waters. However, further research is needed to determine why the ^{13}C-PFOS based approach was insensitive to resolve the previously reported ability of this cyanobacteria species to bio-accumulate PFOS.

2 Introduction

Polyfluoroalkyl substances (PFAS) are synthetic aliphatic compounds that contain strong C–F bonds (Buck et al., 2011). They are manufactured for their favourable amphiphilic properties (possessing both hydrophilic and hydrophobic properties), high thermal resistance, chemical stability and resistance to degradation (Buck et al., 2011; Rahman et al., 2014). Common uses of PFAS are firefighting foams, textile impregnation, electroplating and products with non-stick coatings (Glüge et al., 2020). The continued use of PFAS since the 1940s has led to widespread contamination of various environments including surface waters, groundwater, soils and wastewater, and their presence has even been detected in household dust and agricultural produce (Blake and Fenton, 2020; Shahsavari et al., 2021). PFAS are endocrine disrupting chemicals (EDCs), and as a result of their persistence they can bioaccumulate and cause harm to humans and other organisms when present in excess amounts (Ambaye et al., 2022; Del Fiore et al., 2022). For humans, specific PFAS compounds were shown to have negative effects on thyroid and kidney function as well as on reproduction and fetal development. Exposure to PFAS can further cause liver disease, kidney disease, cancer or adverse immune outcomes such as dyslipidemia (abnormal amount of lipids in blood) (Fenton et al., 2021; Sunderland et al., 2019).

In the Netherlands, a recent report by the Rijksinstituut voor Volksgezondheid en Milieu (RIVM) has documented that the amount of PFAS ingested through drinking water and food exceeds the health-based guidance value (Schepens et al., 2023). This excess human exposure to PFAS is the result of widespread contamination of Dutch soils, groundwaters and surface waters with PFAS. Especially drinking water produced from Dutch surface waters, as opposed to groundwaters, is found to exceed provisional guideline values based on the EFSA (2020) at the majority of locations Sadia et al. (2023). Given that 40% of drinking water in the Netherlands derives from surface waters (Sadia et al., 2023), the implementation of effective and feasible water treatment methods is imperative.

Several technologies have been developed to remediate PFAS contaminated waters. These include adsorption, ion exchange resins, membrane processes, treatment trains, advanced reduction processes and

advanced oxidation processes (Yadav et al., 2022). However, these methods are often expensive, impractical for *in situ* treatment, and require large amounts of energy (Shahsavari et al., 2021). Bio-remediation, which uses organisms to break down PFAS, is an emerging approach that offers a cost-effective alternative to the above list of remediation technologies with the potential for *in situ* treatment. To date, PFAS bio-remediation potential has been investigated for various strains of fungi and bacteria as well as plants (Verma et al., 2021). Research on microbial breakdown of PFAS is largely dominated by studies on soil bacteria (Zhang et al., 2022).

Phototrophic microorganisms are known to utilize a large variety of organic pollutants and offer other advantages such as low nutrient requirements for growth. There has been a growing number of publications on their interaction with PFAS (Hu et al., 2023; Mojiri et al., 2023; Muhammad et al., 2023). Among these studies, four have thus-far been published on the accumulation potential of cyanobacterial and algal species. While two of these studies demonstrated only marginal accumulation rates (Hu et al., 2020; Liao et al., 2024), others identified significant bioaccumulation factors (Mao et al., 2023; Marchetto et al., 2021), suggesting promising potential for bioremediation. For example, the study by Marchetto et al. (2021) showed that the cyanobacterial species *Synechocystis* could remove about 88% of PFOS and 37% of PFOA (Perfluorooctanoic Acid) from solution during growth at PFOS and PFOA concentrations of up to 4 $\mathrm{mg\,L^{-1}}$.

Although these studies demonstrated the potential of cyanobacteria for phyco-remediation of waters contaminated with PFAS, the bio-accumulation potential in all studies was only ascertained based on mass balances of PFAS amounts measured in the culturing medium before and after incubation, PFAS amounts measured after thorough mixing to quantify adsorbed PFAS, and PFAS in solution after artificially induced cell lysis. These studies thereby did not quantify PFOS accumulation through direct measurements of intracellular PFAS content.

This study aimed to develop and apply an approach based on stable isotope probing (SIP) to study accumulation of PFAS by cyanobacteria. The key conceptual idea is that by using ^{13}C-labelled PFOS as a tracer, PFOS bio-accumulation can sensitively be detected by measuring the $^{13}\mathrm{C}/^{12}\mathrm{C}$ isotope ratio in the cyanobacterial biomass, thereby providing a direct quantification of the bio-accumulation factor. PFOS is tested because it is one of the most common long-chain PFAS found in the environment (Umar, 2021). To allow for comparison of results with Marchetto et al. (2021), *Synechocystis* is used as the target cyanobacterial species, and key parameters of the experimental design (incubation period and PFOS concentrations) are in line with Marchetto et al. (2021).

3 Methods

In order to encompass all factors relevant in assessing the potential of *Synechocystis* to accumulate PFOS, this study was approached in two consecutive experiments. In the 1$^{\mathrm{st}}$ experiment, the influence of PFOS on the photosynthetic potential and growth of *Synechocystis* was tested using an ecotoxicological approach. Here, unlabelled PFOS (40 wt% PFOS dissolved in water, sourced from Sigma Aldrich) was used at varying concentrations to determine suitable conditions for the 2$^{\mathrm{nd}}$ experiment. In the 2$^{\mathrm{nd}}$ experiment, the bio-accumulation potential of PFOS was tested through incubating the cyanobacteria with ^{13}C-labelled PFOS (50 $\mathrm{mg\,L^{-1}}$ ($\pm$ 2.5 $\mathrm{mg\,L^{-1}}$); >99% $^{13}\mathrm{C}_8$, sourced from Wellington Laboratories in Canada). This ^{13}C-labelled PFOS inherently comes in solution with methanol. Because it is known that methanol can affect the physiological status of *Synechocystis* (Rigomier et al., 1980), the tolerance of *Synechocystis* to methanol was additionally assessed in a toxicological assay. The aim of this assay was to determine which concentration of ^{13}C-labelled PFOS can be added such that the effect of PFOS can be observed without damaging the cells by methanol.

Culturing and incubation conditions were kept the same across all experiments. *Synechocystis* sp. PCC

6803, sub-strain GT-P, was the wild-type used in experiments, obtained from the laboratory of Prof. Peter Nixon at Imperial College London. The culturing medium used was BG-11. The cultures were grown and incubated at a constant temperature of 28 °C under continuous light. The light intensity was set to 20–25 μmol photons m^{-2} s^{-1}, and the cultures were continuously shaken at a rotational speed of 140 rpm. These conditions differ on some fronts to those used by (Marchetto et al., 2021), where light intensity was set to 150 μmol photons m^{-2} s^{-1} and a temperature of 30 °C was maintained.

3.1 Toxicology assays

Toxicology assays were performed for 7 days in batch cultures containing the BG-11 medium, cyanobacterial inoculum, and PFOS at concentrations of 0, 0.5, 1, 4 and 8 mg L^{-1}. 100 mL Erlenmeyer flasks were used for the incubations with a working volume of 15 mL. Cotton plugs were used to allow for gas exchange with the atmosphere. The starting culture was diluted to an optical density (OD_{720}) of 0.1, and each assay was carried out in triplicate. Daily subsampling into Eppendorf tubes was done in a laminar flow cabinet under sterile conditions.

3.2 Methanol assay

The methanol assay was performed for 7 days considering 3 different treatments: (1) control (no methanol or PFOS), (2) methanol without PFOS and (3) methanol with PFOS. Methanol concentrations corresponding to the amounts present in ^{13}C-PFOS at concentrations of 1 and 4 mg L^{-1} were tested (Table 1). Thereby, batch cultures contained the BG-11 medium, cyanobacterial inoculum, and methanol at concentrations of 0, 16 and 64 mg L^{-1}, in absence and presence of PFOS at corresponding concentrations of 0, 1 and 4 mg L^{-1}. Experiments were carried out in duplicate. In order to simulate the same conditions that were planned for the $^{13}C_8$-PFOS incubations, the starting culture was diluted to an OD_{720} of 0.05, and cultures were incubated in 25 mL Erlenmeyer flasks with a working volume of 4 mL. Cotton plugs were used to allow for gas exchange.

Table 1: PFOS and methanol concentrations [mg L^{-1}] involved in each experiment. For a given ^{13}C-PFOS concentration in the incubation solution, the corresponding methanol concentration was calculated and used in the methanol toxicology.

	Methanol concentration	PFOS concentration
PFOS Toxicology assays	0	0, 0.5, 1, 4, 8
Methanol Toxicology assays	0, 16, 64,	0, 1, 4
$^{13}C_8$-PFOS incubations	0, 16	0, 1

3.3 ^{13}C-PFOS incubation experiment

For stable isotope probing, *Synechocystis* inoculum was incubated with $^{13}C_8$-PFOS at a concentration of 1 mg L^{-1}. This concentration was chosen because (1) the methanol assay revealed that 16 mg L−1 methanol did not have a significant effect on *Synechocystis* growth and photosynthetic potential (Section 4.2), (2) this was the concentration used by Marchetto et al. (2021), allowing for comparison of results, and (3) this concentration was expected to have a measurable effect based on the accumulation capacity of *Synechocystis* derived from Marchetto et al. (2021).

Marchetto et al. (2021) reported that *Synechocystis* specifically removed – and thereby accumulated – 1.72 ± 0.32 mg(PFOS) g^{-1}(biomass) over 2.44 days in a continuous culturing system. Following the general assumption that the carbon content of dry bacterial biomass is 50% (Romanova and Sazhin, 2010), this corresponds to 3.44 ± 0.64 mg(PFOS) g^{-1}(biomass carbon). Given the *Synechocystis* $^{13}C/^{12}C$

ratio of 0.01088 calculated from our own data, this excess ^{13}C incorporation translates to a δ^{13}C value of 59 ‰ over 2.44 days. Calculations followed formulas outlined in equations 1 and 2:

$$R_{sample} = \frac{^{13}C_{biomass} + ^{13}C_{added}}{^{12}C_{biomass}} \tag{1}$$

$$\delta^{13}C_{sample} = \left(\frac{R_{sample}}{R_{standard}} - 1\right) \times 1000 \tag{2}$$

where R_{sample} is the ^{13}C/^{12}C ratio in the sample biomass, $R_{standard}$ is the ^{13}C/^{12}C ratio of the VPDB standard (0.01118), $^{13}C_{biomass}$ represents the moles of original ^{13}C present in the biomass, $^{12}C_{biomass}$ represents the moles of original ^{12}C present in the biomass, and $^{13}C_{added}$ represents the moles of added ^{13}C from PFOS.

To confirm that the expected enrichment would be observed, the presumed amount of ^{13}C-PFOS accumulated by the cells was injected into a control sample of known cell biomass, and measured as a "positive analytical control". This positive analytical control comprised of a tin capsule containing dried control biomass (natural isotope composition), and another tin capsule containing 10 μL of $^{13}C_8$-labelled PFOS, where the methanol was first allowed to evaporate. These were combined into one tin capsule and measured together as one sample. Using the measured carbon content of the dried control biomass, the expected δ^{13}C value was calculated according to equations 1 and 2. This was compared against the measured δ^{13}C.

3.3.1 Bulk Biomass

Two sets of ^{13}C-PFOS incubations were set up for bulk biomass analysis. Biomass was collected using two sampling methods, centrifugation and filtering. One 7 day incubation series was subsampled for biomass using centrifugation, after 10 min and 7 days. Another 4 day incubation series was subsampled for biomass using filtration, after 10 min, 2 days and 4 days. The last time point of each incubation series was sampled using both methods, to enable method comparison. The incubation series were started from different *Synechocystis* cultures, and the starting culture of each experiment was used as the respective "control" for that experiment. Each $^{13}C_8$-PFOS incubation series was carried out in triplicate. The starting cultures were diluted to an OD_{720} of 0.05, and cultures were incubated in 25 mL Erlenmeyer flasks with a working volume of 4 mL.

For the centrifugation method, samples were centrifuged at 4000 rpm for 15 minutes, after which the supernatant was poured off. The cells were washed with an equivalent volume of ultrapure water, where the pellet was homogenized through gently pipetting up and down. The washed cells were re-centrifuged under the same conditions and the supernatant discarded. It was microscopically confirmed that the cells were not lysed in these steps. The remaining biomass was transferred to a tin cup and oven-dried at 65 °C for 24 hours. For the filtration method, samples were filtered using single-use syringes and pre-combusted Whatman GF-F filters (pore size 0.7 μm). Filters were oven-dried at 65 °C for an hour, acidified using 150 μL HCl, and oven-dried for additional 4 hours.

3.3.2 Individual cell level

An additional ^{13}C-PFOS incubation was set up for individual cell analysis using nanoSIMS. A single incubation was subsampled in triplicate for biomass after 10 min, 3 days and 5 days and 7 days. Biomass was harvested through dropping 50 μL suspended culture onto an Au-coated polycarbonate filter (pore size 0.2 μm), and allowing filtrate to absorb into underlying filter paper. The filters were moved to clean filter paper and washed four times with an equivalent volume of ultrapure water.

3.4 Analytical procedures

During the toxicology assays, cell counts and cell sizes were measured daily using a Beckman Coulter Multisizer 4 Coulter Counter, operated using a 30 μm aperture set to detect cells within a size range of 1.25–3 μm. F_v/F_m and OD was measured daily using the AquaPen-P AP-P 100, a handheld fluorometer. Cell count and OD values on day 0 were measured only for the starting culture, and were calculated for other PFOS concentrations according to the dilution factor as a result of PFOS addition. AquaPen F_v/F_m samples were dark-adapted for 5 minutes prior to measurements and measured using blue excitation light (455 nm). Chlorophyll *a* and carotenoid concentrations were measured for the starting culture and at the end of the experiment using a Thermo Spectronic UV 5000 UV/VIS spectrophotometer, following the procedure outlined by Zavřel et al. (2015). At the same time points, the cultures were additionally analysed using Fast Repetition Rate Fluorometry (FRRF), which exposes samples to light pulses of increasing intensity through which several response attributes were measured (Table 2). Cultures were dark adapted for 10 minutes, and 30 μL culture was diluted with 1.97 mL BG-11. LED excitation light was set to 450 and 624 nm in equal shares. The photomultiplier tube gain was set to 330 V.

Table 2: Photosynthetic variables measured by FRRF.

Fv	variable fluorescence
Fm	maximum fluorescence
F_v/F_m	Dark adapted maximum quantum yield of PSII
F_v'/F_m'	Light adapted maximum quantum yield of PSII
NPQ	non-photochemical quenching
σ	photosystem II functional absorption cross section

For the ^{13}C-PFOS incubation experiment, $^{13}C/^{12}C$ ratios in the bulk biomass samples were determined using EA-IRMS. Samples were introduced into a Thermo Scientific Flash IRMS EA IsoLink System coupled via a Thermo Scientific CONFLO IV universal continuous flow interface to a Thermo Scientific DELTA V Advantage isotope ratio mass spectrometer. Centrifuged samples containing a range of 26 to 261 μg C were diluted 50% using helium gas through the continuous flow interface to remain within the voltage detection limit. Filtered samples were not diluted and contained a range of 26 to 67 μg C. IAEA-CH-7 and nicotinamide were used as laboratory standards between samples, and a graphite-quartz laboratory standard was used at the start of the run to enable accurate determination of sample carbon content. The analytical uncertainty was determined as the standard deviation of nicotinamide measurements. All values are reported as δ^{13}C relative to the VPDB standard, unless otherwise stated.

$^{13}C/^{12}C$ ratios on a single cell level were determined using the NanoSIMS 50L instrument (Cameca) operated at Utrecht University. NanoSIMS analysis allows visualisation of the spatial distribution of $^{13}C/^{12}C$ ratios within individual cells (Polerecky et al., 2021). If PFOS were accumulated, nanoSIMS imaging would therefore enable determination of cell structures incorporating $^{13}C_8$-PFOS. Using a 16 KeV Cs^+ primary ion beam, the nanoSIMS instrument was set to multi-collection mode to simultaneously detect negative secondary ions $^{19}F^-$, $^{12}C^-$, $^{13}C^-$, $^{12}C_2$, $^{12}C^{13}C^-$, $^{12}C^{14}N^-$ and $^{31}P^-$, alongside secondary electron imaging. The mass spectrometer was tuned with sufficient resolution ($\gtrsim$ 6000) to be able to separate ^{13}C from ^{12}CH peaks and $^{12}C^{13}C$ from $^{12}C_2H$ peaks on the nominal masses 13 and 25, respectively, allowing determination of $^{13}C/^{12}C$ ratios from the ion count ratios in two ways: $^{13}C^-/^{12}C^-$ and $0.5 \cdot {}^{12}C^{13}C^-/({}^{12}C_2^- + 0.5 \cdot {}^{12}C^{13}C^-)$. Samples were pre-sputtered prior to analysis (Cs^+ implanted) through rastering a defocused primary ion beam with a high current in absence of a diaphragm until a point of signal intensity stabilization. Images were processed and analysed using LANS (Look@NanoSIMS) software run in Matlab (Polerecky et al., 2012). NanoSIMS images were analysed through defining regions of interest (ROIs) that correspond to cell clusters or cell-free areas on a filter. Cell clusters were defined based on $^{12}C^{14}N$ images, where cells were clearly visible in contrast to the filter (Section 4.3.2, Fig. 9a).

In order to increase the signal to noise ratio in analysing stable isotope ratios, cells were highlighted and analysed as clusters of between 4 and 15 cells.

3.5 Statistical analysis

All statistical analyses were performed in R Statistical Software version 4.3.2 (R Core Team, 2021). Differences between growth rates at varying PFOS concentrations were assessed using linear mixed effects models (LMM) on log-transformed cell densities within the exponential growth phase, implemented using the nlme package (Pinheiro et al., 2023). The exponential phase was visually determined to lie between 0—3 days. The model considered time and PFOS concentrations as fixed variables, and the biological replicate as a random variable. Given that sample variance increased over time, sample contribution to LME fitting was weighted according to time. The slope of the LMM is representative of the growth rate. Differences between growth rates at varying PFOS concentrations were assessed through comparing slopes of individual linear fits for each biological replicate, using a one way ANOVA (analysis of variance).

Differences between growth rates at varying PFOS concentrations were additionally assessed using logistical growth models, defined according to equation 3, and solved in R using the ode function in the deSolve package (Soetaert et al., 2010). The carrying capacity (k), growth rate (r) and initial cell count were fitted to observed data for each biological replicate, using the modCost and modFit functions in the FME package (Soetaert and Petzoldt, 2010). Growth rates were compared using a one way ANOVA.

$$\frac{dCellcount}{dtime} = r \times Cellcount \times \left(1 - \frac{Cellcount}{k}\right) \tag{3}$$

At single time points, differences between variables at varying PFOS concentrations were assessed through a one-way ANOVA test. The underlying assumptions of ANOVA were tested prior to its employment, and the test was only applied where these assumptions had been met. Normality was assessed visually, through QQ-plots and using the Shapiro-Wilk test, and the equality of variances was tested both visually and through Levene's test. These statistical analyses were implemented in R, using the Companion to Applied Regression package (Fox and Weisberg, 2019). At single time points where differences between variables at only two PFOS concentrations were compared, T-student tests were applied. All graphics were produced using the ggplot2 package (Wickham, 2016).

4 Results

4.1 Toxicology assays

Cell counts and OD measurements indicated that the exponential growth phase occurred in the first 3 days, followed by the stationary phase from day 5 to day 7. *Synechocystis* growth rates determined using LMM decreased with increasing PFOS concentration (Fig. 1). For growth rates derived from cell counts, this effect was significant ($p = 0.0039$) but small, corresponding to a 6.8% decrease in growth rate for the highest PFOS concentration (8 $\mathrm{mg\,L^{-1}}$) compared to the control. For growth rates derived from OD measurements, the effect was not significant ($p = 0.2333$). There was a significant difference in initial cell densities, which was attributed to the dilution of cultures by varying volumes of PFOS.

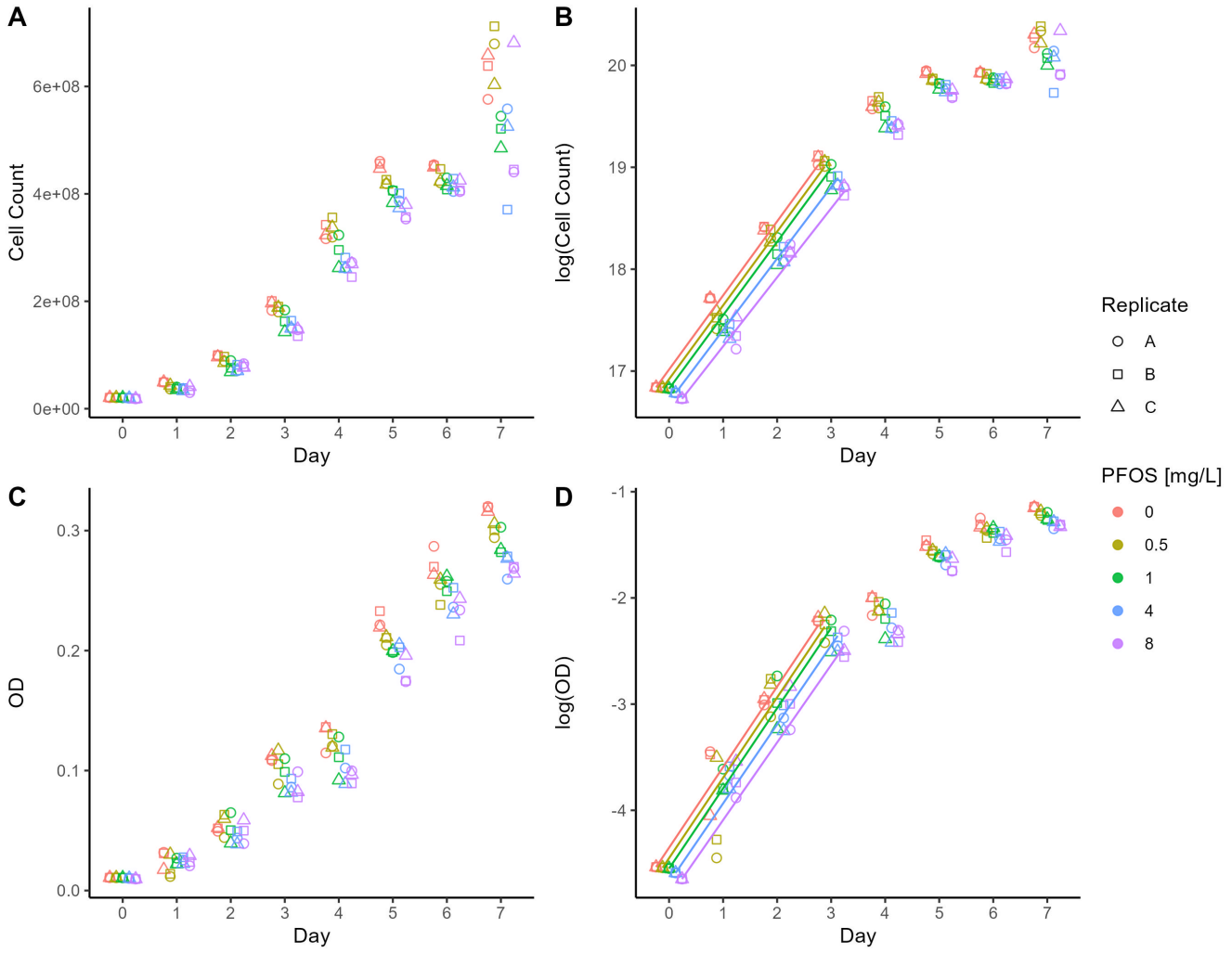

Figure 1: Effects of PFOS on growth of *Synechocystis* in batch cultures. Shown are (a) cell counts, (b) optical densities and log transformations of these ((c) and (d) respectively) as a function of time measured in triplicate culturing bottles. Lines represent the fitted linear mixed model for each PFOS concentration during the exponential growth phase (coefficients shown in Supplementary Tables S1 and S2). Horizontal jitter between points measured at the same time point was applied to improve visualisation. Cell count uncertainty, determined as the standard deviation of repeated measurements, was $\pm\ 4 \times 10^6$ cells.

Growth rates determined from the linear fits (of log-transformed cell counts) decreased slightly with increasing PFOS concentration (Fig. 2). There was a 5.3% decrease in growth rate for the highest PFOS concentration (8 $\mathrm{mg\,L^{-1}}$) compared to the control. However, the effect of PFOS was not significant ($p = 0.078$). There was additionally no significant effect of PFOS on growth rates determined from logistic growth models, and no clear trend (Fig. 2). The majority of statistical analyses therefore showed no significant effect of PFOS on growth rate, and where they were significant, they were very small.

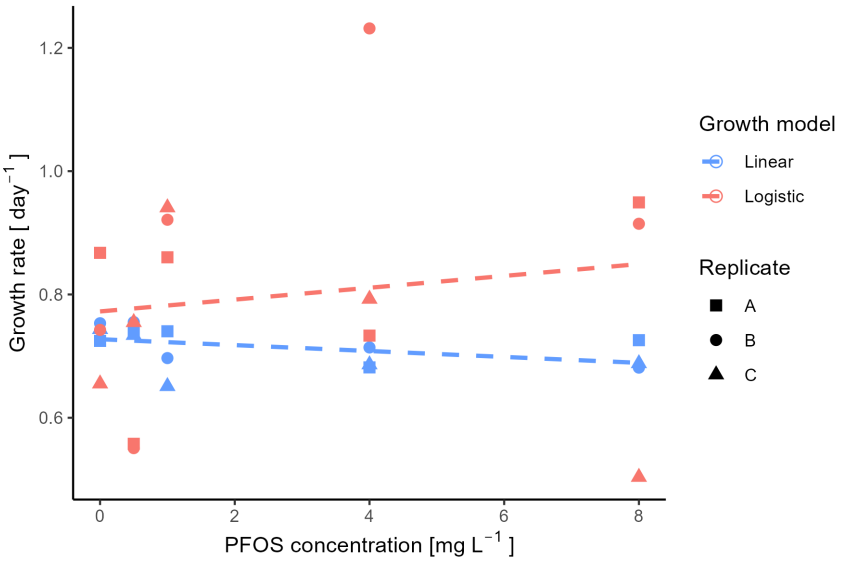

Figure 2: Effects of PFOS on growth rates of *Synechocystis* in batch cultures. Shown are growth rates determined from fitted logistic growth models (red), and from the slope of linearly fitted log-transformed cell counts in the exponential growth phase (blue). Growth rates were determined separately for each biological replicate. Shown lines of best-fit have equations (1) $0.772 + 0.0096 \times PFOS$ and (2) $0.727 - 0.00479 \times PFOS$ for logistic and linear growth models respectively.

Within the first 4 days of incubation, there was a minor but significant positive trend between cell size and PFOS concentration ($p<0.0001$) (Fig. 3a). This trend was absent from day 5 to day 7. There was a minor but significant ($p<2\times10^{-16}$) increase in cell size from day 5 to day 7, of $\sim$0.2 μm.

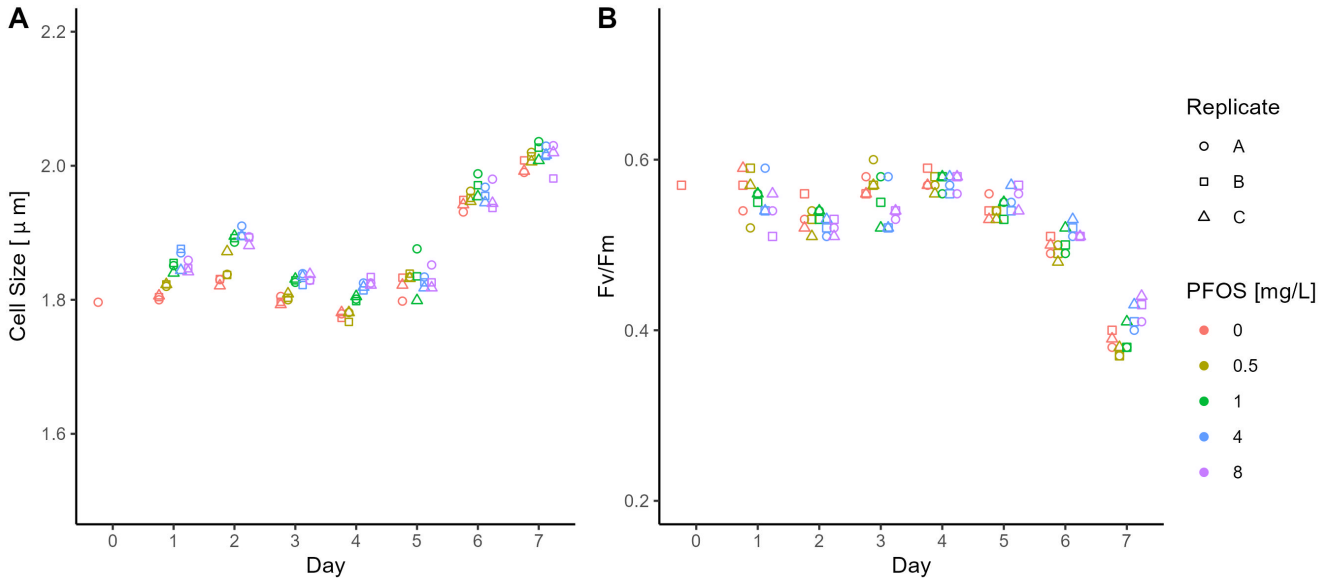

Figure 3: Effects of PFOS on *Synechocystis* (a) cell size and (b) F_v/F_m (determined using the Aquapen-P AP-P100 device), for cultures incubated with PFOS at concentrations ranging between 0–8 mg L^{-1}. Horizontal jitter between points measured at the same time point was applied to improve visualisation.

The AquaPen instrument revealed that the F_v/F_m ratios were between 0.51—0.6 within the first 5 days.

This decreased to ratios between 0.37—0.44 on the 7th day (Fig. 3b). The FRRF instrument revealed that the F_v/F_m ratios were between 0.15—0.21 on the 7th day. There was no significant difference between F_v/F_m ratios in control cells and those incubated in PFOS concentrations of 8 mg L^{-1} ($p = 0.389$) on the 7th day. Light adapted F'_v/F'_m, which corresponds to the maximum quantum yield of PSII in the light if all reaction centres are open, was slightly but significantly higher for cells incubated in PFOS concentrations of 8 mg L^{-1} compared to control cells ($p = 0.0011$).

Table 3: Photosynthetic parameters derived from FRRF measurements of *Synechocystis* cells, measured for the control and PFOS incubations at a concentration of 8 mg L^{-1} after 7 days of growth. The photosynthetically active radiation (PAR) light intensity [μmol photons m^{-2} s^{-1}] is specified for each measurement.

PFOS	PAR 0	PAR 20	PAR 0	PAR 20	PAR 1207
	F_v/Fm	F'_v/F'_m	$\boldsymbol{\sigma}$		**NPQ**
0 mg L^{-1}	0.167	0.0516	3.640	4.022	0.47
	0.164	0.0511	3.635	4.325	0.45
	0.164	0.0500	3.607	4.050	0.42
8 mg L^{-1}	0.151	0.0730	3.583	4.317	
	0.183	0.06551	3.387	3.682	0.40
	0.212	0.06941	3.256	4.288	0.45

Additional parameters determined by FRRF on day 7 showed no significant differences between the control and cells incubated with PFOS at concentrations of 8 mg L^{-1}. These parameters include NPQ – indicative of the dissipation of energy into heat – at the highest light intensity, and σ – representative of photosystem II functional absorption cross sections – at the light intensity used throughout incubations (PAR 20 units), and in dark adapted samples.

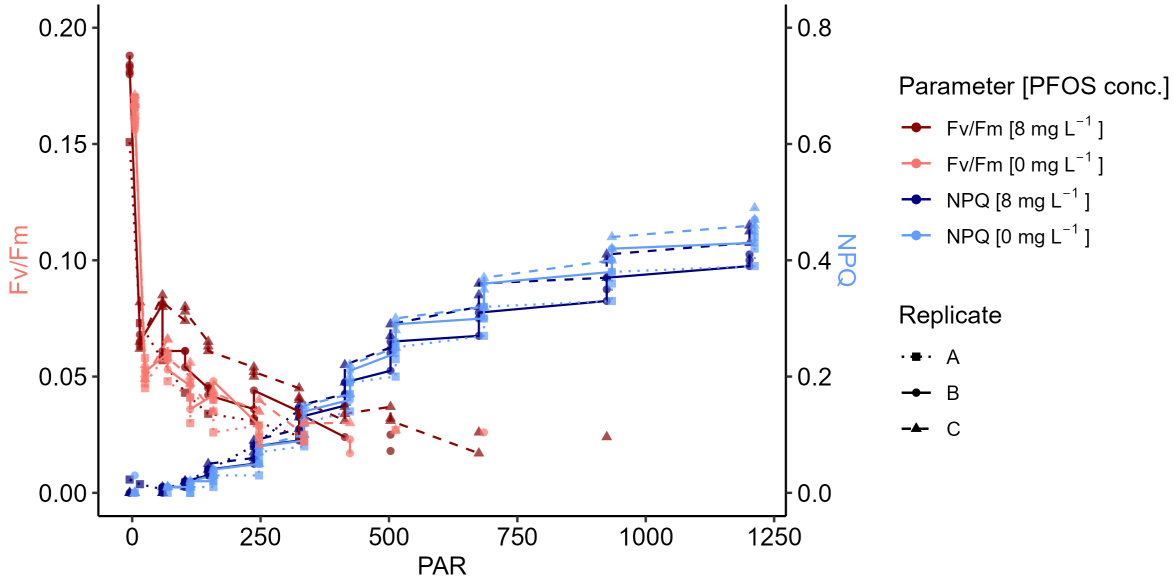

Figure 4: Light curves showing F_v/F_m and NPQ for the control cultures [0 mg L^{-1}] and cultures incubated with PFOS at 8 mg L^{-1}, measured by FRRF. Horizontal jitter between points measured at the same time point was applied to improve visualisation.

Chlorophyll *a* and carotenoid concentrations measured on the 7^{th} day of incubation revealed no statistically significant difference ($p = 0.322$ and 0.545, respectively) between cells incubated at the tested PFOS concentrations between 0–8 mg L^{-1} (Fig. 5). Chlorophyll *a* and carotenoid concentrations of the starting cultures measured on day 0 were 77 and 32 fg $cell^{-1}$. Thereby, chlorophyll a and carotenoid content decreased 7-fold from that measured in the starting culture on day 0 to that on day 7 across all PFOS concentrations.

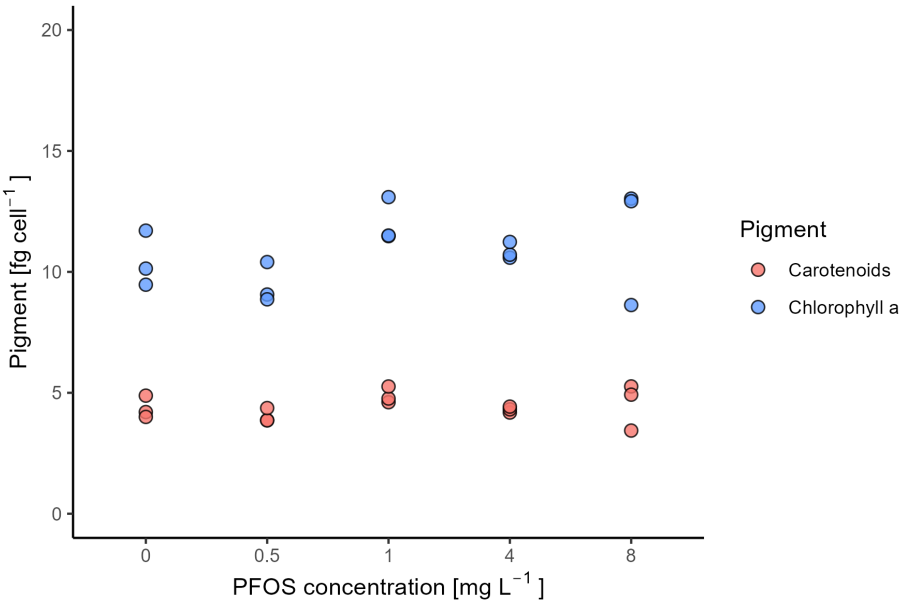

Figure 5: Chlorophyll *a* and carotenoid content per cell for *Synechocystis* incubated for 7 days with PFOS at concentrations ranging between 0–8 mg L^{-1}. Measurement uncertainty, determined as the standard deviation of repeated measurements, was ± 0.015 fg $cell^{-1}$.

4.2 Methanol Toxicology

For cultures incubated with methanol at a concentration of 16 mg L^{-1} for 7 days, cell counts increased at a rate similar to the control (Fig. 6). For cultures incubated with methanol at a concentration of 64 mg L^{-1}, cell counts decreased over the measured period of 3 days (Fig. 6). *Synechocystis* cells formed clusters when incubated with the higher methanol concentration (64 mg L^{-1}), irrespective of the presence or absence of PFOS (Supplementary Fig. S1). Cell size decreased for cultures incubated at the higher methanol concentration (64 mg L^{-1}), suggesting only single cells, and no clusters, were measured. For cultures incubated with the lower methanol concentration (16 mg L^{-1}) for 7 days, cell size increased at a similar rate to the control (Fig. 7). Therefore, methanol at a concentration of 64 mg L^{-1} negatively affected cell count and cell size of *Synechocystis*, while methanol at 16 mg L^{-1} did not have a noticeable effect.

F_v/F_m ratios for cultures incubated with methanol were variable over the measured time-points across 7 days (Fig. 7). F_v/F_m was lower in samples incubated with methanol within an hour after its addition to the culture compared to control cultures. On day 3 only cultures incubated with the higher concentration of methanol (64 mg L^{-1}) yielded comparatively lower values of F_v/F_m, and on day 7 all samples (controls and methanol incubations) show comparable F_v/F_m values. Therefore, the data did not exhibit any clear trends that could be interpreted.

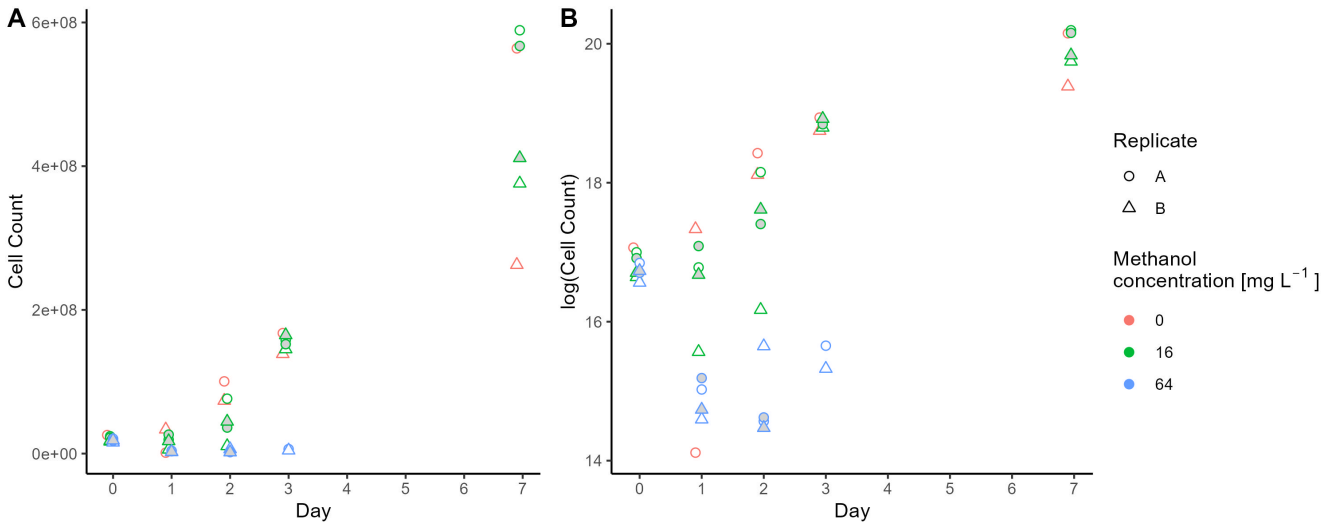

Figure 6: Effect of methanol on growth of *Synechocystis* in batch cultures. Shown are (a) cell counts and (b) log cell counts of *Synechocystis* incubated with methanol at concentrations of 16 and 64 mg L^{-1}, in the absence (white fill) and presence (grey fill) of PFOS at corresponding concentrations of 1 and 4 mg L^{-1}. Cell counts on day 7 are missing for incubations with a methanol concentration of 64 mg L^{-1}, as the cell counter aperture was repetitively blocked. Aperture blockage was likely caused by the formation of clusters under high methanol concentrations.

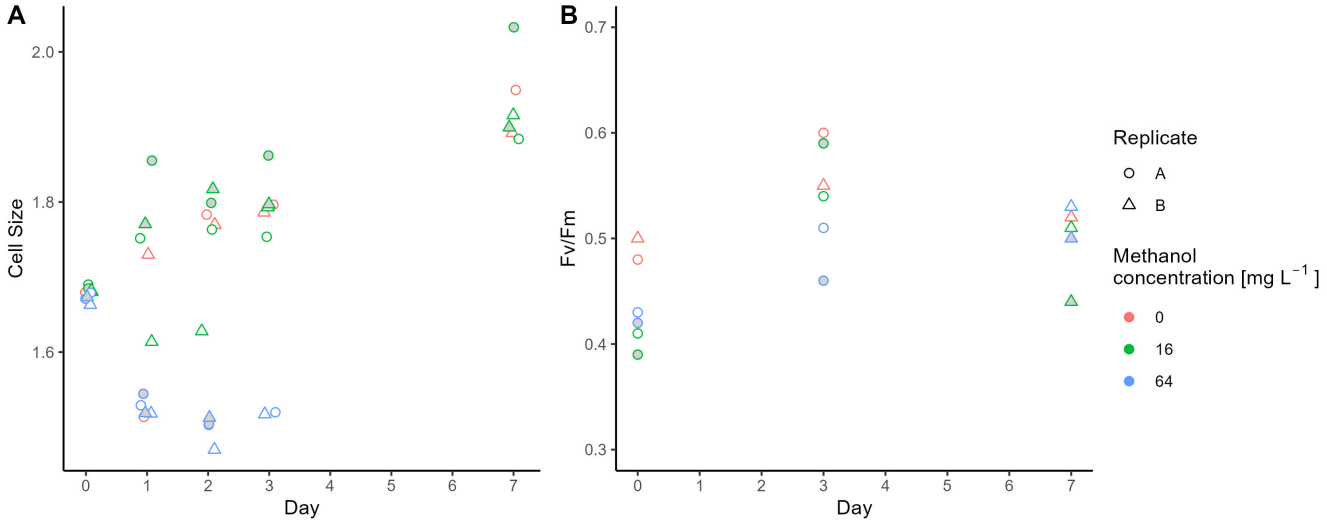

Figure 7: Effect of methanol on *Synechocystis* (a) cell size and (b) F_v/F_m ratios of *Synechocystis* in batch cultures. Cultures were incubated with methanol at concentrations of 16 and 64 mg L^{-1}, in the absence (white fill) and presence (grey fill) of PFOS at corresponding concentrations of 1 and 4 mg L^{-1}. Horizontal jitter between points measured at the same time point was applied to improve visualisation. Again, cell counts on day 7 are missing for incubations with a methanol concentration of 64 mg L^{-1}, as the cell counter aperture was repetitively blocked.

In conclusion, these results show that the effect of methanol is negligible at the lower tested concentration of 16 mg L^{-1}. This methanol concentration corresponds to that present in ^{13}C-PFOS concentrations of 1 mg L^{-1}, and this treatment was therefore selected for the ^{13}C-PFOS incubations.

4.3 ^{13}C-PFOS incubations

4.3.1 Bulk biomass

Based on PFOS accumulation rates in *Synechocystis* derived from Marchetto et al. (2021), we expected to see a δ^{13}C value of 59 ‰ over 2.44 days. Instead, a general decreasing trend was observed in δ^{13}C relative to the control, for *Synechocystis* incubated with ^{13}C-PFOS at a concentration of 1 mg L^{-1} (Fig. 8a). At the end of the incubations, mean δ^{13}C values of -2.61 ± 0.40 ‰ and -7.44 ± 0.36 ‰ were observed for incubation series lasting 4 and 7 days respectively (centrifuged samples, Fig. 8a). Prior to the decreasing trend, a small increase in δ^{13}C was observed after 10 minutes of incubation, of 2.62 ± 0.40 ‰ (7 day experiment) and 6.10 ± 1.99 ‰ (4 day experiment). The former was sampled using centrifugation and the latter was sampled using filtration. Incubations sampled using centrifugation yielded consistently lower, and less variable, δ^{13}C values than the same samples measured using filtration (days 4 and 7, Fig 8a). *Synechocystis* incubated with methanol at a concentration of 64 mg L^{-1} for 3 days yielded a mean δ^{13}C of -3.58 ± 0.25 ‰ relative to the control.

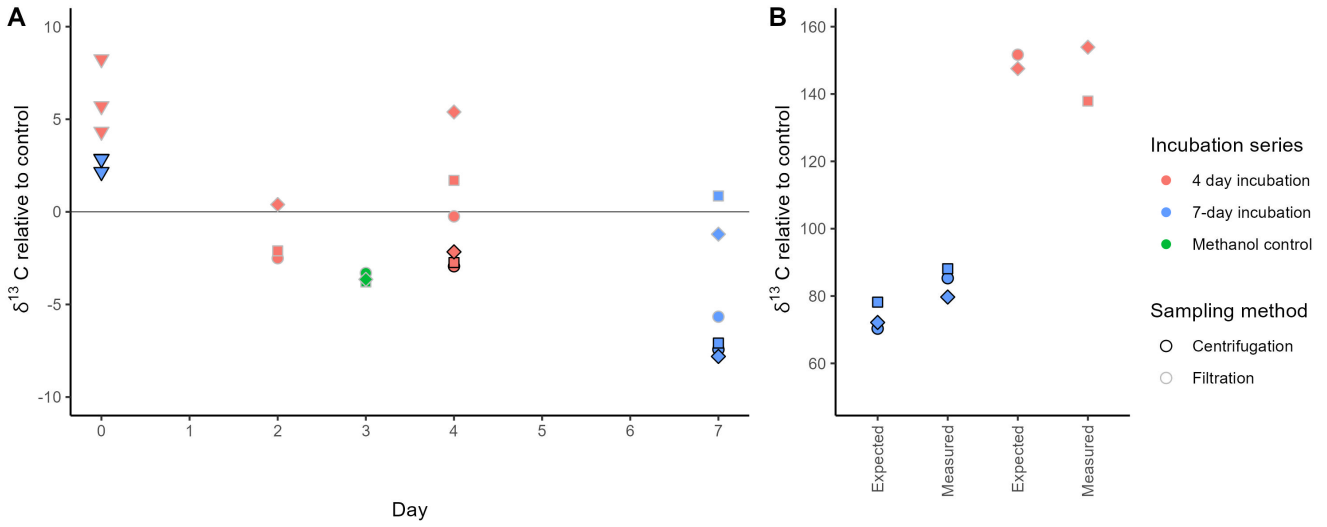

Figure 8: δ^{13}C of ^{13}C-PFOS-incubated samples, methanol-incubated controls and positive analytical controls. Panel (a) shows the bulk biomass δ^{13}C relative to the respective control of each incubation series, plotted together with the methanol-incubated control. Aside from day 0 samples which were taken from separate incubations, the same shape within each experiment indicates the same biological replicate. Panel (b) shows the measured and expected δ^{13}C of the positive analytical controls. The analytical uncertainty associated with measurements was ± 0.036 ‰.

The positive control for the longer incubation series (7 days) showed an enrichment of 70.3–78.2 ‰ relative to the control biomass (Fig. 8b). Based on mass-balance calculations (as described in Section 3.3), the expected enrichment for this incubation series was between 79.7–88.1 ‰. The measured enrichment was higher than the expected enrichment for the centrifuged samples, possibly due to inaccurate pipetting (about 10% error). The positive control for the shorter incubation series (4 days) showed an enrichment of 137.9–153.9 ‰ relative to the control biomass. This corresponded relatively well to the expected enrichment of 147.5–161.9 ‰ (Fig. 8b).

The controls of each incubation series differed by approximately 6.6 ‰ (Table 4), where the 4 and 7 day incubation series had mean δ^{13}C values relative to VPDB of -33.2 and -26.6 ‰, respectively.

Table 4: Control $\delta^{13}C$ [‰] values relative to VPDB standard for the 4 and 7 day incubation series. Methanol controls used the same starting culture as the 4 day incubation, thus also the same control.

4 day incubation	7 day incubation
−32.81	−26.70
−33.55	−26.53
−36.82	−26.54

4.3.2 NanoSIMS

Whilst variability in data across each treatment is on the level of analytical precision of NanoSIMS, to optimise accuracy and allow for comparison of different treatments, the cell $^{13}C/^{12}C$ data was corrected for instrument drift as observed in filter measurements. NanoSIMS images showed that there was a lower carbon signal in cells relative to the filter (Fig. 9b and c), and not much difference between filters and

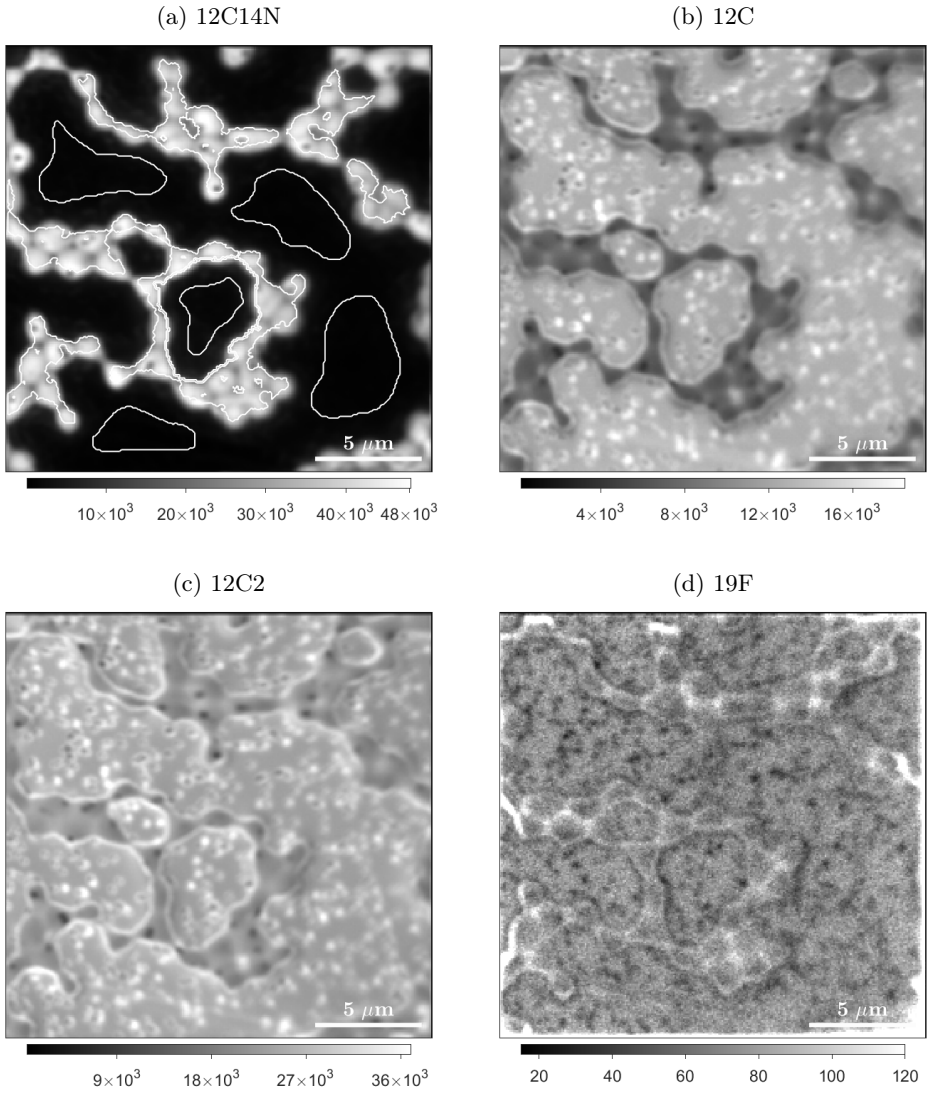

Figure 9: Representative examples of secondary ion count images obtained by NanoSIMS from *Synechocystis* cells placed on a polycarbonate filter. Panel (a) shows outlines of ROIs corresponding to cell clusters or filter areas.

cells with respect to the fluorine ion counts (Fig. 9d). Whilst cells displayed in Fig. 9 were incubated with $^{13}C_8$-PFOS for 5 days, these patterns were similar for measured cells collected at all time points, including those collected after 10 mins and 7 days.

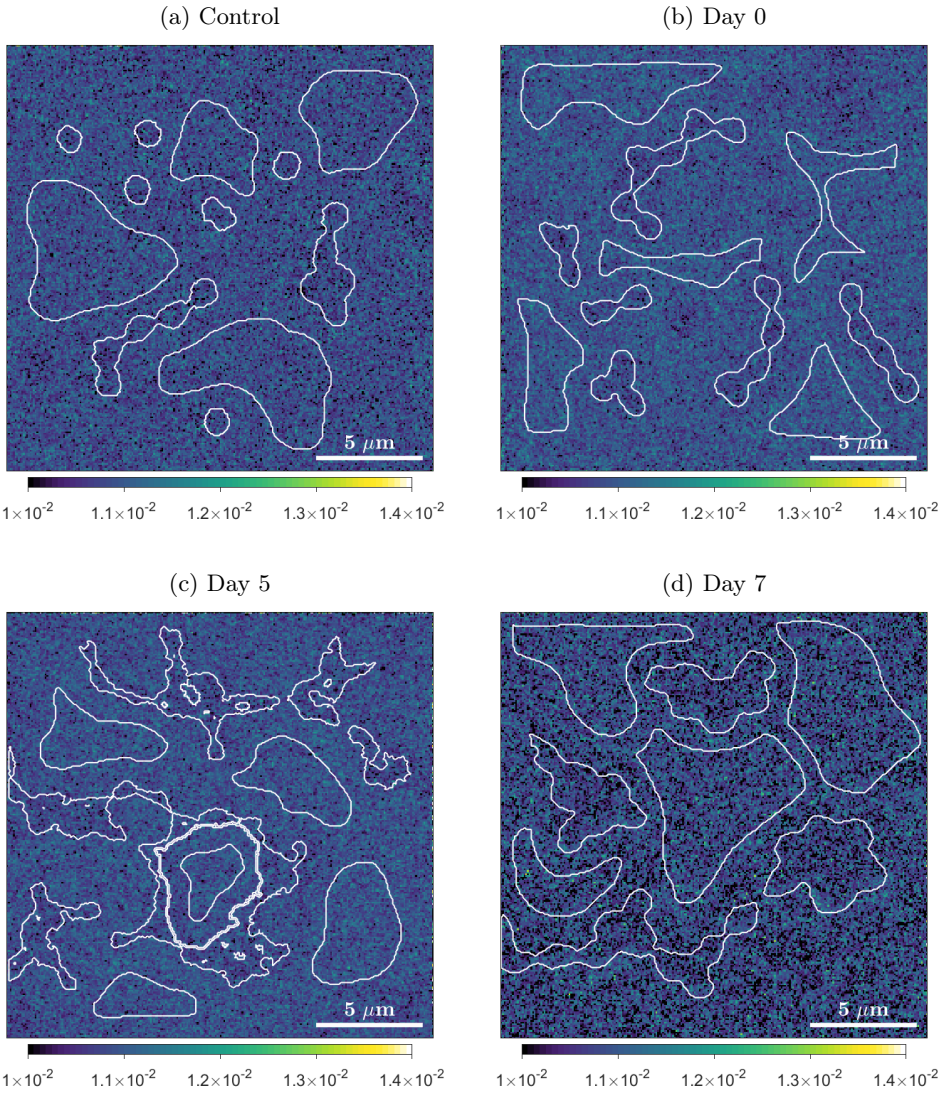

Figure 10: Distribution of $^{13}C/^{12}C$ ratios in the *Synechocystis*cells after (b) 10 minutes, (c) 5 days and (d) 7 days of incubation with 1 mg L^{-1} ^{13}C-PFOS.

Similarly to bulk analyses, nanoSIMS analysis revealed a decrease in $\delta^{13}C$ relative to the control when incubated with ^{13}C-PFOS, in the same range as $\delta^{13}C$ values observed for bulk biomass analysis. NanoSIMS samples taken after 10 minutes of incubation had similar $\delta^{13}C$ values to the control biomass. Interestingly, lowest $\delta^{13}C$ values were observed on day 5, the only treatment that was statistically significantly different from the control. Incubations sampled on day 5 had a mean $\delta^{13}C$ value of -5.28 ± 2.34‰. $\delta^{13}C$ increased slightly from day 5 to day 7. Day 7 yielded a mean $\delta^{13}C$ value of -2.23 ± 1.98‰.

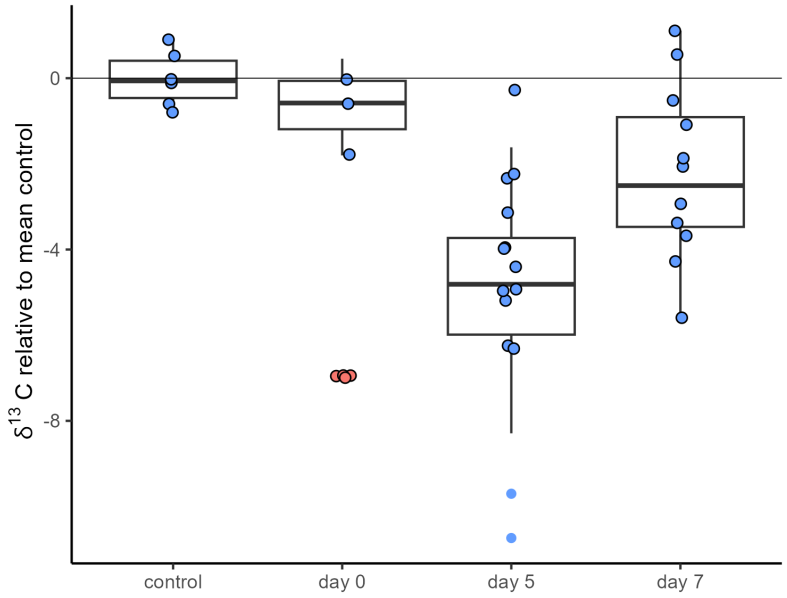

Figure 11: δ^{13}C relative to the mean control for nanoSIMS samples taken after 10 minutes, 5 days and 7 days of incubation in a PFOS concentration of 1 mg L^{-1}. Red points are thought to belong to day 0 but it is unsure whether they have been misidentified. Individual data-points correspond to clusters of cells, in order to increase the signal to noise ratio.

5 Discussion

5.1 PFOS toxicology

Growth rate is an important variable in bacterial toxicity testing (Bitton and Koopman, 1992) and a key determinant of cell culture health. We found that the growth rate of *Synechocystis* was not significantly affected by PFOS at concentrations of 0.5, 1, 4 and 8 mg L^{-1} incubated for 7 days, as determined from the majority of statistical analyses. The only significant effect of PFOS on *Synechocystis* was observed in LMM analysis of cell counts, and this effect was deemed to be small. These result align with findings by Marchetto et al. (2021), who observed no significant effect of PFOS on *Synechocystis* growth rate determined from OD. However, experiments by Marchetto et al. (2021) were limited to PFOS concentrations of up to 1 mg L^{-1} and an incubation time of 4 days, whereas our study explored PFOS concentrations of up to 8 mg L^{-1} and an incubation time of 7 days.

The lack of significant differences between variables indicative of photosynthetic potential measured in the control culture and cultures incubated with PFOS at a concentration of 8 mg L^{-1} after 7 days of incubation, suggests that the photosynthetic potential of *Synechocystis* is not significantly affected by the presence of PFOS in solution. The effects of PFOS on *Synechocystis* health assessed by Marchetto et al. (2021) were limited to respirometric tests – measurement of oxygen production and consumption – up to maximum PFOS concentrations of 4 mg L^{-1}. Our study goes one step further, and determines photosynthetic health through the use of FRRF, AquaPen fluorometry and essential photosynthetic pigments, up to PFOS concentrations of 8 mg L^{-1}.

Various aspects of *Synechocystis* physiological status have an effect on PSII functional cross sections (Dubinsky, 1992). No significant difference between values of functional cross sections (σ) were found, indicating that the physiology of the cyanobacterial cells remains largely unaltered in the presence of a PFOS concentration of 8 mg L^{-1}. Non-photochemical quenching (NPQ) is essential in dissipating harmful excess

excitation energy in photosynthetic membranes of cyanobacteria (Schulze and Caldwell, 2012), thereby avoiding damage to the PSII reaction center (Ruban, 2016). Comparison of NPQ between incubations revealed that PFOS (at 8 mg L^{-1}) does not have a significant effect on non-photochemical quenching.

The lack of significant differences between photosynthetic pigment concentrations (both chlorophyll *a* and carotenoids) at different PFOS concentrations measured after 7 days of incubation, additionally suggests that the physiology of the cyanobacterial cells was not significantly affected by the presence of PFOS in solution at concentrations between 0.5 and 8 mg L^{-1}. Carotenoids have various functions within cyanobacteria. They play a role in light harvesting, photoprotection, elimination of oxidative stress and contribute to the structure of thylakoid membranes (Schagerl and Müller, 2006; Zhu et al., 2010). Their concentration within cyanobacteria varies considerably under changing growth conditions, and they are key physiological and structural indicators, such that lower carotenoid concentrations are frequently associated with higher cellular stress levels (Zavřel et al., 2015). Chlorophyll *a* plays a role in light harvesting as well as in the conversion of energy from absorbed photons to chemical energy. The combined assessment of chlorophyll *a* and carotenoid pigment concentrations thereby give useful insights into the physiological state of cyanobacterial cells (Zavřel et al., 2015), which were in this study determined to be unaffected by PFOS.

Comparison of F_v/F_m between dark-adapted incubations revealed that PFOS (at 8 mg L^{-1}) does not have a significant effect on F_v/F_m, which represents the maximum quantum yield of PSII and is therefore an indicator of the health of the photosynthetic apparatus (Assunção et al., 2022). In light adapted samples at the incubation light intensity of 20 μmol photons m^{-2} s^{-1}, higher observed F'_v/F'_m in samples incubated with 8 mg L^{-1} could be attributed to the higher dilution of these samples at the start of the incubations. Although the observed effect was small, lower cell densities present in 8 mg L^{-1} flasks relative to the control could have resulted in lower nutrient limitation and reduced cell shading. Thereby, 8 mg L^{-1} incubations possibly had slightly lower cell stresses compared to the control, which would explain the higher F'_v/F'_m ratios observed in these incubations.

Values of F_v/F_m found in healthy cyanobacterial cultures are usually in the range of 0.5–0.7 (Santabarbara et al., 2019), and whilst F_v/Fm measured using the AquaPen fluorometer fall into this range in the first 6 days, the 7^{th} day yields lower ratios (0.37–0.44). F_v/F_m ratios measured using FRRF of the control and 8 mg L^{-1} samples on the 7^{th} day lie in the range of 0.15–0.21, lower than those measured using the AquaPen device. The significant decrease in F_v/F_m observed across all PFOS concentrations in days 6–7 of the incubation coincide with an increased cell size, and the transition towards the stationary phase. These are indications of cellular stress, and could be attributed to two processes. One hypothesis is that increasing cell density results in self-shading of cells, where the average exposure to light decreases from the perspective of a single cell (Posten, 2009). Decreased light exposure may result in reduced assimilation of carbon through photosynthesis, and can be reflected in slower cell growth and decreased F_v/F_m. A second hypothesis is that the observed behaviour is the direct result of a nutrient limitation, which is frequently the cause for low F_v/F_m ratios (Sánchez-Zurano et al., 2021; He et al., 2015). Nutrient limitation is a plausible stressor, given that batch cultures start with a limited un-replenishable nutrient supply which restricts the duration of the exponential growth phase. Given the additional stresses across all treatments – either from cell shading or nutrient limitation as an inherent effect of using batch experiments – it is possible that the observation of additional effects by PFOS was prevented, as these were outweighed by greater stressors. Thereby, these stresses could have compromised the interpretation of results in days 6—7 of the experiment.

The focus of this study was on determining the effects of PFOS on specific indicators of cellular health, including growth rate and photosynthetic potential. We found no significant effect of PFOS with concentrations of up to 8 mg L^{-1} on any of the measured indicators. This, however, does not necessarily mean that there is no adverse effect of PFOS on the cells' health status. Other indicators, such as viability,

ATP, oxygen uptake or heat production could be affected by contaminants such as PFOS (Bitton and Koopman, 1992), but were not measured in this study. Nevertheless, the largely unaltered cellular health upon exposure to PFOS revealed from the parameters measured in this study, demonstrates *Synechocystis* resilience to high concentrations of PFOS (up to 8 $mg\,L^{-1}$). This novel finding, in combination with the suggested PFOS accumulation potential of *Synechocystis* (Marchetto et al., 2021), provided sufficient motivation to further investigate the bio-accumulation potential of *Synechocystis* in this study.

5.2 ^{13}C PFOS incubations

Our study aimed to reproduce the accumulation rates reported by Marchetto et al. (2021) through stable isotope probing, a novel method that would allow direct quantification of the amount of PFAS in the biomass, as opposed to frequently employed indirect measurements that rely on changes in solution PFAS, cell lysis, and washing of cells for quantification of adsorbed PFAS (Hu et al., 2020; Liao et al., 2024; Marchetto et al., 2021; Presentato et al., 2020). Contrary to the expected enrichment of 59 ‰ over 2.44 days (Section 3.3), the experimental data in the present study does not show an enrichment in ^{13}C within the bulk biomass, which would be indicative of the expected PFOS accumulation. In light of this, our experiments do not confirm the hypothesis that *Synechocystis* accumulates PFOS.

The δ^{13}C of the analytical positive control matches the expected enrichment, suggesting that any accumulation of ^{13}C-PFOS by the cells during incubations should be reflected in bulk biomass measurements. This suggests that the only way in which accumulation did occur but was not measured, is through "escape" of PFOS during sample preparation. Whilst it was microscopically determined that cells were not lysed during centrifugation, oven drying could have resulted in some volatilisation of PFOS. However, the volatility of PFOS is low, with a vapor pressure of only 0.0078 kPa at the applied drying temperatures of 65°C (derived using the Clausius-Clapeyron relationship and data from Bastow et al. (2022)), meaning the rate of PFOS evaporation would be relatively slow. Additionally, volatilisation would not have affected any PFOS integrated in the cell membrane, and it was suggested by Marchetto et al. (2021) that 49 % of the accumulated PFOS was incorporated in the cell membrane after incubation with PFOS concentrations of 1 $mg\,L^{13}$ in batch experiments lasting 4 days. This suggests that even if all PFOS in the cell lysate was vaporised, 49% of the expected ^{13}C enrichment through ^{13}C-PFOS accumulation should still be measured. Since this was not measured, this suggests that PFOS was in fact not accumulated, and not incorporated into the cell membrane.

The PFOS accumulation rate reported by Marchetto et al. (2021) was determined using a continuous flow experiment. Whilst batch experiments were also employed, PFOS accumulation rates were not determined for these (Marchetto et al., 2021). Batch experiments, as used in our study, result in nutrient limitation and variable biomass concentration over time, which could prevent the complete acclimation of the cells. Changes in cell growth rates may in turn affect the removal rate of PFOS by the cells. Therefore, accumulation rates derived from batch experiments could possibly be lower than those derived from continuous flow experiments. Marchetto et al. (2021) reported that *Synechocystis* in batch experiments removed 71% of PFOS, compared to the 88% removed in continuous cultivation systems. Therefore, the lower accumulation rate in batch experiments would still lead to a significant enrichment if the corresponding amount of ^{13}C-PFOS was accumulated. Thereby, based on our findings it appears that accumulation of PFOS did not occur.

In the absence of ^{13}C-PFOS accumulation, the observed variability in δ^{13}C within the cell biomass may be due to effects of methanol or PFOS on the kinetic fractionation associated with carbon fixation by the RuBisCO enzyme. The observed ~7.4 ‰ and ~2.5 ‰ decrease (7^{th} day) in δ^{13}C relative to the control in the bulk biomass and nanoSIMS measurements respectively, could be a result of changing environmental and subsequently physiological conditions in the presence of methanol or PFOS, which has been shown to produce fractionation variability in the cyanobacterial biomass Garcia et al. (2023).

The enzymatic fixation of CO_2 by RuBisCO accounts for essentially all carbon fixation by photosynthetic organisms, and in doing so preferentially fixates $^{12}CO_2$ (Sharkey and Berry, 1985). The intrinsic discrimination against ^{13}C results in the natural depletion of ^{13}C in organic carbon relative to that found in inorganic carbon of the environment, leading to a mean deviation of around −25 ‰ (Guy et al., 1993; Kędzior et al., 2022; Roeske and O'Leary, 1984). Cyanobacteria possess a CO_2 concentrating mechanism (CCM) which enhances CO_2 concentration in the vicinity of RuBisCO and maximises the ratio between CO_2 and the competitive inhibitor O_2 (Huffine et al., 2023). In cyanobacteria there exist several CMM components. Carboxysomes form distinct cellular compartments containing RuBisCO, with protein shells that form a CO_2 diffusion barrier such that CO_2 can accumulate (Espie and Kimber, 2011). Transformation of HCO_3^- to CO_2 within the carboxysome is accelerated by carbonic anhydrase, and uptake of CO_2 is facilitated by NDH-1_4 (Eichner, 2014; Eichner et al., 2015). The overall fractionation during photosynthesis can be altered by factors which affect the local environment of the carboxylation reaction (Sharkey and Berry, 1985), and cause changes in the carbon isotope ratio within the carboxysome carbon pool. Leakiness is defined as the ratio of CO_2 efflux to gross inorganic carbon uptake. If leakage is low, the intracellular carbon pool is less frequently refreshed, such that RuBisCO is forced to additionally use $^{13}CO_2$ as a carbon source, and the discrimination of RuBisCO against ^{13}C cannot be fully expressed. Increased leakage allows the intracellular carbon pool to be refreshed, meaning the isotope ratio of the intracellular carbon pool becomes similar to the outside carbon pool, which allows RuBisCO fractionation to be more strongly expressed. Additionally, HCO_3^- is 7.9 ‰ enriched in ^{13}C relative to CO_2 (Sharkey and Berry, 1985), such that a relative increase in the use of CO_2 as a carbon source would lead to a decrease in the biomass $\delta^{13}C$.

Studies have shown that the photosynthetic carbon isotope fractionation may vary as a result of environmental factors and physiological responses of the cell, including pH, temperature, growth rate, CO_2 concentration, light, and nutrient availability (Bidigare et al., 1997; Eek et al., 1999; Eichner et al., 2015; Hurley et al., 2021; Laws et al., 1995; Roeske and O'Leary, 1984; Wong and Sackett, 1978). Varying environmental conditions may lead to varying carbon isotope discrimination as a result of changes in the leakiness of the cells, the species of DIC transported and the rate of DIC transport (Sharkey and Berry, 1985). It is possible that altered cell physiology as a result of ^{13}C-PFOS or methanol in solution increased the leakage factor, or increased the relative contribution of CO_2 as a carbon source for fixation, leading to a reduction in $\delta^{13}C$ in the bulk biomass with increased incubation time.

Amphiphilic properties enable PFOS molecules to partition into cellular membranes, allowing disruption of membrane properties. Various studies on the impact of PFAS on microbial membranes and functions show that PFAS partitioning into membranes results in increased fluidity and permeability (Fitzgerald, 2017; Fitzgerald et al., 2018a,b; Naumann et al., 2022). Increased membrane permeability and fluidity may allow for enhanced diffusion of CO_2 into and out of the cell, such that the leakage factor increases and RuBisCO fractionation can be more strongly expressed. However, the incorporation of ^{13}C-labelled PFOS in the membrane would in itself cause an increase in $\delta^{13}C$, and if ^{13}C-PFOS was accumulated in the amounts as suggested by Marchetto et al. (2021), we should see a clear enrichment in ^{13}C which would outweigh the additional fractionation.

A study by Rigomier et al. (1980) on the effect of methanol on *Bacillus subtilis* showed that the total cellular content of phospholipids was reduced by 50% and synthesis of phosphatidylglycerol (lipid with a function in regulating cell membrane permeability) was strongly inhibited in the presence of methanol. Increased membrane fluidity during exposure to alcohols has been documented to increase leakage across the membrane (Huffer et al., 2011). Through the same mechanism, enhanced diffusion of carbon sources across the membrane would allow RuBisCO fractionation to be more strongly expressed. This hypothesised mechanism is supported by our data, where the methanol-incubated control exhibited the same behaviour as ^{13}C-PFOS-incubated samples, with a mean $\delta^{13}C$ of −3.58 ‰ after 3 days of incubation. This is thereby a possible mechanism for the reduction in biomass ^{13}C seen under exposure to the methanol in which

$^{13}C_8$-PFOS is dissolved.

5.3 Areas for future work

The present study does not find any accumulation of ^{13}C-PFOS through direct measurement of the cellular biomass $^{13}C/^{12}C$ ratios. This contradicts findings by Marchetto et al. (2021), who indirectly derived accumulation of PFOS through measuring cell lysis and incubation solution PFOS concentrations. Therefore, whether PFOS is accumulated and where it is accumulated within the *Synechocystis* cell remains unconfirmed. Further research is required to draw conclusive results about the accumulation potential of *Synechocystis*. The study by Marchetto et al. (2021) covered an indirect approach of measuring PFOS accumulation, whilst this study attempted direct measurement of PFOS in the cyanobacterial biomass. Additional research should be carried out using multiple methods of PFOS measurement with the aim of 100% recovery. Thereby, a closed ^{13}C-PFOS incubation should be sampled for solution, headspace and biomass. The PFOS content should be measured within each, and ^{13}C enrichment should be determined within each carbon pool. Additionally, methods used by Marchetto et al. (2021), UHPLC coupled to HRMS, should be employed to ascertain PFOS concentrations in solution and lysate and compare results to those obtained through stable isotope probing from the same incubations. This would allow a direct comparison of methods and enable us to ascertain where the discrepancy between results in this study and that by Marchetto et al. (2021) originate from.

Additionally, given the significant effect of methanol on cyanobacteria, future work using ^{13}C-labelled PFOS should aim to incubate the biomass with ^{13}C-PFOS supplied not as dissolved in methanol but rather as a salt or a solution in water.

6 Conclusion

In this study, *Synechocystis* was shown to tolerate PFOS concentrations up to the maximum tested concentration of 8 mg L^{-1}. Growth rate and various photosynthetic variables – F_v/F_m, $F'_v/F'm$, σ, NPQ, chlorophyll *a* and carotenoid content – indicative of the physiology and photosynthetic health of the cell, were unaffected by the presence of PFOS during the exponential and stationary phase of the cell cycle. These findings underscore the resilience of *Synechocystis* to PFOS-induced stresses, boding well for its potential use in bio-remediation

However, in contrast to the expected increase in δ^{13}C as a result of ^{13}C-PFOS accumulation, we observed a small but significant decrease in δ^{13}C in bulk biomass. A small decrease in δ^{13}C was additionally observed in nanoSIMS data, suggesting that PFOS was not accumulated by the cells. This finding contradicts previously reported results, where bio-accumulation was observed through indirect measurements, considering PFOS concentrations in solution and cell lysate. Thereby, whether PFOS is accumulated by *Synechocystis* remains unconfirmed, and the reason for the discrepancy between these two studies remains unclear. Further research is required to determine why the ^{13}C-PFOS based approach is insensitive to resolve the previously reported bio-accumulation potential of this cyanobacteria.

Acknowledgements

This research was supported by the Olaf Schuiling fonds of Utrecht University Fund. I extend my gratitude to the Centre Algatech, Institute of Microbiology, a division of the Czech Academy of Sciences, for providing access to their facilities, which was instrumental in conducting my experiments.

I especially want to thank my supervisors Lubos Polerecky and Meri Eichner for their support and guidance during this project. Their mentorship and expertise were invaluable throughout the duration of my thesis.

I would additionally like to thank Michiel Kienhuis and Desmond Eefting for their valuable support with NanoSIMS and EA-IRMS analysis.

References

Ambaye, T. G., Vaccari, M., Prasad, S., and Rtimi, S. (2022). Recent progress and challenges on the removal of per-and poly-fluoroalkyl substances (PFAS) from contaminated soil and water. *Environmental Science and Pollution Research*, 29(39):58405–58428.

Assunção, J., Pagels, F., Tavares, T., Malcata, F. X., and Guedes, A. C. (2022). Light Modulation for Bioactive Pigment Production in Synechocystis salina. *Bioengineering*, 9(7):331.

Bastow, T. P., Douglas, G. B., and Davis, G. B. (2022). Volatilization Potential of Per- and Poly-fluoroalkyl Substances from Airfield Pavements and during Recycling of Asphalt. *Environmental Toxicology and Chemistry*, 41(9):2202–2208.

Bidigare, R. R., Fluegge, A., Freeman, K. H., Hanson, K. L., Hayes, J. M., Hollander, D., Jasper, J. P., King, L. L., Laws, E. A., Milder, J., Millero, F. J., Pancost, R., Popp, B. N., Steinberg, P. A., and Wakeham, S. G. (1997). Consistent fractionation of 13C in nature and in the laboratory: Growth-rate effects in some haptophyte algae. *Global Biogeochemical Cycles*, 11(2):279–292.

Bitton, G. and Koopman, B. (1992). Bacterial and Enzymatic Bioassays for Toxicity Testing in the Environment. In *Reviews of Environmental Contamination and Toxicology: Continuation of Residue Reviews*, Reviews of Environmental Contamination and Toxicology, pages 1–22. Springer, New York, NY.

Blake, B. E. and Fenton, S. E. (2020). Early life exposure to per-and polyfluoroalkyl substances (PFAS) and latent health outcomes: A review including the placenta as a target tissue and possible driver of peri-and postnatal effects. *Toxicology*, 443:152565.

Buck, R. C., Franklin, J., Berger, U., Conder, J. M., Cousins, I. T., De Voogt, P., Jensen, A. A., Kannan, K., Mabury, S. A., and van Leeuwen, S. P. (2011). Perfluoroalkyl and polyfluoroalkyl substances in the environment: terminology, classification, and origins. *Integrated environmental assessment and management*, 7(4):513–541.

Del Fiore, P., Cavallin, F., Mazza, M., Benna, C., Monico, A. D., Tadiotto, G., Russo, I., Ferrazzi, B., Tropea, S., and Buja, A. (2022). Per-and polyfluoroalkyl substances (PFAS) exposure in melanoma patients: a retrospective study on prognosis and histological features. *Environmental Health*, 21(1):126.

Dubinsky, Z. (1992). The Functional and Optical Absorption Cross-Sections of Phytoplankton Photosynthesis. In *Primary Productivity and Biogeochemical Cycles in the Sea*, pages 31–45. Springer US, Boston, MA.

Eek, M. K., Whiticar, M. J., Bishop, J. K. B., and Wong, C. S. (1999). Influence of nutrients on carbon isotope fractionation by natural populations of Prymnesiophyte algae in NE Pacific. *Deep Sea Research Part II: Topical Studies in Oceanography*, 46(11):2863–2876.

Eichner, M. (2014). *Process-understanding of marine nitrogen fixation under global change*. PhD thesis, Universität Bremen.

Eichner, M., Thoms, S., Kranz, S. A., and Rost, B. (2015). Cellular inorganic carbon fluxes in tri-

chodesmium: a combined approach using measurements and modelling. *Journal of experimental botany*, 66(3):749–759.

Espie, G. S. and Kimber, M. S. (2011). Carboxysomes: cyanobacterial rubisco comes in small packages. *Photosynthesis Research*, 109:7–20.

Fenton, S. E., Ducatman, A., Boobis, A., DeWitt, J. C., Lau, C., Ng, C., Smith, J. S., and Roberts, S. M. (2021). Per-and polyfluoroalkyl substance toxicity and human health review: Current state of knowledge and strategies for informing future research. *Environmental toxicology and chemistry*, 40(3):606–630.

Fitzgerald, N. (2017). *Impact of Perfluoroalkyl Substances on Microbial Membranes and Microbial Functions*. PhD thesis, University of Minnesota.

Fitzgerald, N. J. M., Simcik, M. F., and Novak, P. J. (2018a). Perfluoroalkyl Substances Increase the Membrane Permeability and Quorum Sensing Response in Aliivibrio fischeri. *Environmental Science & Technology Letters*, 5(1):26–31.

Fitzgerald, N. J. M., Wargenau, A., Sorenson, C., Pedersen, J., Tufenkji, N., Novak, P. J., and Simcik, M. F. (2018b). Partitioning and Accumulation of Perfluoroalkyl Substances in Model Lipid Bilayers and Bacteria. *Environmental Science & Technology*, 52(18):10433–10440.

Fox, J. and Weisberg, S. (2019). *An R Companion to Applied Regression*. Sage, Thousand Oaks CA, third edition.

Garcia, A. K., Kędzior, M., Taton, A., Li, M., Young, J. N., and Kaçar, B. (2023). Effects of RuBisCO and CO2 concentration on cyanobacterial growth and carbon isotope fractionation. *Geobiology*, 21(3):390–403.

Glüge, J., Scheringer, M., Cousins, I. T., DeWitt, J. C., Goldenman, G., Herzke, D., Lohmann, R., Ng, C. A., Trier, X., and Wang, Z. (2020). An overview of the uses of per-and polyfluoroalkyl substances (PFAS). *Environmental Science: Processes & Impacts*, 22(12):2345–2373.

Guy, R. D., Fogel, M. L., and Berry, J. A. (1993). Photosynthetic Fractionation of the Stable Isotopes of Oxygen and Carbon. *Plant Physiology*, 101(1):37–47.

He, Q., Yang, H., Wu, L., and Hu, C. (2015). Effect of light intensity on physiological changes, carbon allocation and neutral lipid accumulation in oleaginous microalgae. *Bioresource Technology*, 191:219–228.

Hu, J., Wang, D., Zhang, N., Tang, K., Bai, Y., Tian, Y., Li, Y., and Zhang, X. (2023). Effects of perfluorooctanoic acid on Microcystis aeruginosa: Stress and self-adaptation mechanisms. *Journal of Hazardous Materials*, 445:130396.

Hu, Y., Meng, F.-L., Hu, Y.-Y., Habibul, N., and Sheng, G.-P. (2020). Concentration-and nutrient-dependent cellular responses of microalgae chlorella pyrenoidosa to perfluorooctanoic acid. *Water Research*, 185:116248.

Huffer, S., Clark, M. E., Ning, J. C., Blanch, H. W., and Clark, D. S. (2011). Role of alcohols in growth, lipid composition, and membrane fluidity of yeasts, bacteria, and archaea. *Applied and environmental microbiology*, 77(18):6400–6408.

Huffine, C. A., Zhao, R., Tang, Y. J., and Cameron, J. C. (2023). Role of carboxysomes in cyanobac-

terial CO2 assimilation: CO2 concentrating mechanisms and metabolon implications. *Environmental Microbiology*, 25(2):219–228.

Hurley, S. J., Wing, B. A., Jasper, C. E., Hill, N. C., and Cameron, J. C. (2021). Carbon isotope evidence for the global physiology of Proterozoic cyanobacteria. *Science Advances*, 7(2):eabc8998.

Kędzior, M., Garcia, A. K., Li, M., Taton, A., Adam, Z. R., Young, J. N., and Kaçar, B. (2022). Resurrected Rubisco suggests uniform carbon isotope signatures over geologic time. *Cell Reports*, 39(4):110726.

Laws, E. A., Popp, B. N., Bidigare, R. R., Kennicutt, M. C., and Macko, S. A. (1995). Dependence of phytoplankton carbon isotopic composition on growth rate and [CO2]aq: Theoretical considerations and experimental results. *Geochimica et Cosmochimica Acta*, 59(6):1131–1138.

Liao, J., Sun, B., Wang, C., Cao, Z., Wu, Z., An, X., Liang, Z., Huang, X., and Lu, Y. (2024). Uptake and cellular responses of *Microcystis aeruginosa* to PFOS in various environmental conditions. *Ecotoxicology and Environmental Safety*, 272:116041.

Mao, W., Li, M., Xue, X., Cao, W., Wang, X., Xu, F., and Jiang, W. (2023). Bioaccumulation and toxicity of perfluorooctanoic acid and perfluorooctane sulfonate in marine algae *Chlorella sp. Science of The Total Environment*, 870:161882.

Marchetto, F., Roverso, M., Righetti, D., Bogialli, S., Filippini, F., Bergantino, E., and Sforza, E. (2021). Bioremediation of per-and poly-fluoroalkyl substances (PFAS) by synechocystis sp. PCC 6803: a chassis for a synthetic biology approach. *Life*, 11(12):1300.

Mojiri, A., Nazari Vishkaei, M., Ansari, H. K., Vakili, M., Farraji, H., and Kasmuri, N. (2023). Toxicity Effects of Perfluorooctanoic Acid (PFOA) and Perfluorooctane Sulfonate (PFOS) on Two Green Microalgae Species. *International Journal of Molecular Sciences*, 24(3):2446.

Muhammad, F. S., Chia, M. A., Abolude, D. S., Tanimu, S., and Otogo, R. A. (2023). Growth, antioxidant response and microcystin production by Microcystis aeruginosa exposed to the surfactant perfluorooctanesulfonic acid (PFOS). *Phycologia*, 62(3):259–267.

Naumann, A., Alesio, J., Poonia, M., and Bothun, G. D. (2022). PFAS fluidize synthetic and bacterial lipid monolayers based on hydrophobicity and lipid charge. *Journal of Environmental Chemical Engineering*, 10(2):107351.

Pinheiro, J., Bates, D., and R Core Team (2023). *nlme: Linear and Nonlinear Mixed Effects Models*. R package version 3.1-164.

Polerecky, L., Adam, B., Milucka, J., Musat, N., Vagner, T., and Kuypers, M. M. M. (2012). Look@NanoSIMS – a tool for the analysis of nanoSIMS data in environmental microbiology. *Environmental Microbiology*, 14(4):1009–1023.

Polerecky, L., Masuda, T., Eichner, M., Rabouille, S., Vancová, M., Kienhuis, M. V., Bernát, G., Bonomi-Barufi, J., Campbell, D. A., and Claquin, P. (2021). Temporal patterns and intra-and inter-cellular variability in carbon and nitrogen assimilation by the unicellular cyanobacterium Cyanothece sp. ATCC 51142. *Frontiers in Microbiology*, 12:620915.

Posten, C. (2009). Design principles of photo-bioreactors for cultivation of microalgae. *Engineering in Life Sciences*, 9(3):165–177.

Presentato, A., Lampis, S., Vantini, A., Manea, F., Daprà, F., Zuccoli, S., and Vallini, G. (2020). On

the Ability of Perfluorohexane Sulfonate (PFHxS) Bioaccumulation by Two Pseudomonas sp. Strains Isolated from PFAS-Contaminated Environmental Matrices. *Microorganisms*, 8(1):92.

R Core Team (2021). *R: A Language and Environment for Statistical Computing*. R Foundation for Statistical Computing, Vienna, Austria.

Rahman, M. F., Peldszus, S., and Anderson, W. B. (2014). Behaviour and fate of perfluoroalkyl and polyfluoroalkyl substances (PFASs) in drinking water treatment: A review. *Water research*, 50:318–340.

Rigomier, D., Bohin, J. P., and Lubochinsky, B. (1980). Effects of ethanol and methanol on lipid metabolism in Bacillus subtilis. *Journal of general microbiology*, 121(1):139–149.

Roeske, C. and O'Leary, H. (1984). Carbon isotope effects on enzyme-catalyzed carboxylation of ribulose bisphosphate. *Biochemistry*, 23(25):6275–6284.

Romanova, N. D. and Sazhin, A. F. (2010). Relationships between the cell volume and the carbon content of bacteria. *Oceanology*, 50(4):522–530.

Ruban, A. V. (2016). Nonphotochemical Chlorophyll Fluorescence Quenching: Mechanism and Effectiveness in Protecting Plants from Photodamage. *Plant Physiology*, 170(4):1903–1916.

Sadia, M., Nollen, I., Helmus, R., ter Laak, T. L., Béen, F., Praetorius, A., and van Wezel, A. P. (2023). Occurrence, Fate, and Related Health Risks of PFAS in Raw and Produced Drinking Water. *Environmental Science & Technology*, 57(8):3062–3074.

Santabarbara, S., Villafiorita Monteleone, F., Remelli, W., Rizzo, F., Menin, B., and Casazza, A. P. (2019). Comparative excitation-emission dependence of the FV/FM ratio in model green algae and cyanobacterial strains. *Physiologia Plantarum*, 166(1):351–364.

Schagerl, M. and Müller, B. (2006). Acclimation of chlorophyll *a* and carotenoid levels to different irradiances in four freshwater cyanobacteria. *Journal of Plant Physiology*, 163(7):709–716.

Schepens, M. A. A., te Biesebeek, J. D., Hartmann, J., van der Aa, N., Zijlstra, R., and Boon, P. E. (2023). Risk assessment of exposure to PFAS through food and drinking water in the Netherlands. *RIVM rapport 2023-0011*.

Schulze, E.-D. and Caldwell, M. M. (2012). *Ecophysiology of Photosynthesis*. Springer Science & Business Media.

Shahsavari, E., Rouch, D., Khudur, L. S., Thomas, D., Aburto-Medina, A., and Ball, A. S. (2021). Challenges and current status of the biological treatment of PFAS-contaminated soils. *Frontiers in Bioengineering and Biotechnology*, 8:602040.

Sharkey, T. D. and Berry, J. A. (1985). Carbon isotope fractionation of algae influenced by an inducible CO2-concentrating mechanism. *Inorganic carbon uptake by aquatic photosynthetic organisms. s. Rockville: American Society of Plant Physiologists.*, pages 389–401.

Soetaert, K. and Petzoldt, T. (2010). Inverse Modelling, Sensitivity and Monte Carlo Analysis in R Using Package FME. *Journal of Statistical Software*, 33:1–28.

Soetaert, K., Petzoldt, T., and Setzer, R. W. (2010). Solving Differential Equations in R: Package deSolve. *Journal of Statistical Software*, 33:1–25.

Sunderland, E. M., Hu, X. C., Dassuncao, C., Tokranov, A. K., Wagner, C. C., and Allen, J. G. (2019). A

review of the pathways of human exposure to poly-and perfluoroalkyl substances (PFASs) and present understanding of health effects. *Journal of exposure science & environmental epidemiology*, 29(2):131–147.

Sánchez-Zurano, A., Lafarga, T., Morales-Amaral, M. d. M., Gómez-Serrano, C., Fernández-Sevilla, J. M., Acién Fernández, F. G., and Molina-Grima, E. (2021). Wastewater treatment using Scenedesmus almeriensis: Effect of operational conditions on the composition of the microalgae-bacteria consortia. *Journal of Applied Phycology*, 33:3885–3897.

Umar, M. (2021). Reductive and Oxidative UV Degradation of PFAS—Status, Needs and Future Perspectives. *Water*, 13(22):3185.

Verma, S., Varma, R. S., and Nadagouda, M. N. (2021). Remediation and mineralization processes for per-and polyfluoroalkyl substances (PFAS) in water: a review. *Science of The Total Environment*, 794:148987.

Wickham, H. (2016). *ggplot2: Elegant Graphics for Data Analysis*. Springer-Verlag New York.

Wong, W. W. and Sackett, W. M. (1978). Fractionation of stable carbon isotopes by marine phytoplankton. *Geochimica et Cosmochimica Acta*, 42(12):1809–1815.

Yadav, S., Ibrar, I., Al-Juboori, R. A., Singh, L., Ganbat, N., Kazwini, T., Karbassiyazdi, E., Samal, A. K., Subbiah, S., and Altaee, A. (2022). Updated review on emerging technologies for PFAS contaminated water treatment. *Chemical Engineering Research and Design*, 182:667–700.

Zavřel, T., Sinetova, M., and Červený, J. (2015). Measurement of Chlorophyll a and Carotenoids Concentration in Cyanobacteria. *Bio-protocol*, 5(9).

Zhang, Z., Sarkar, D., Biswas, J. K., and Datta, R. (2022). Biodegradation of per-and polyfluoroalkyl substances (PFAS): A review. *Bioresource technology*, 344:126223.

Zhu, Y., Graham, J. E., Ludwig, M., Xiong, W., Alvey, R. M., Shen, G., and Bryant, D. A. (2010). Roles of xanthophyll carotenoids in protection against photoinhibition and oxidative stress in the cyanobacterium *Synechococcus* sp. strain PCC 7002. *Archives of Biochemistry and Biophysics*, 504(1):86–99.

Supplementary Materials

Table S1: LME coefficients and statistics for cell count data in the exponential growth phase ($\leq$ 3 days) for cultures incubated with PFOS concentrations of 0–8 mg L^{-1}.

	Coefficient	Std. Error	p-value
Intercept	16.841125	0.000211960	0.000000000
Day	0.726900	0.008216611	0.000000000
PFOS	−0.014097	0.000052581	0.000000000
Day:PFOS	−0.006218	0.002038290	0.003901785

LME analysis suggests that the log-transformed cell count varies over time and different PFOS concentrations according to the following formula:

$$log[CellCount] = (16.84 - 0.0141 \cdot PFAS) + (0.727 - 0.0062 \cdot PFAS) \cdot Day$$

Table S2: LME coefficients and statistics for OD data in the exponential growth phase ($\leq$ 3 days) for cultures incubated with PFOS concentrations of 0–8 mg L^{-1}.

	Coefficient	Std. Error	p-value
Intercept	−4.533883	0.000211963	0.0000000
Day	0.758426	0.011687963	0.000000000
PFOS	−0.014097	0.000052582	0.000000000
Day:PFOS	−0.003505	0.002899427	0.2333078

LME analysis suggests that the log-transformed OD varies over time and different PFOS concentrations according to the following formula:

$$log[OD] = (-4.534 - 0.0141 \cdot PFAS) + (0.758 - 0.0035 \cdot PFAS) \cdot Day$$

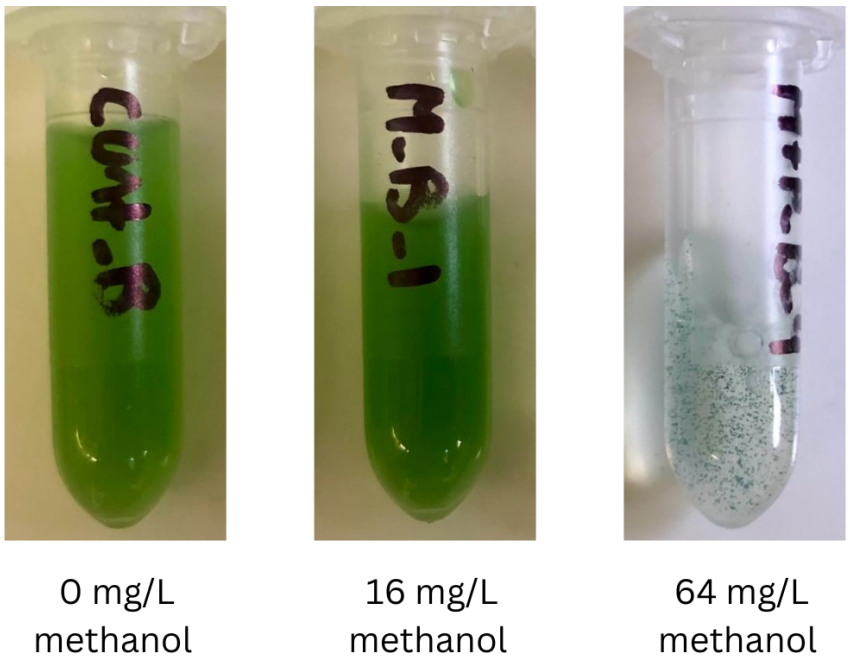

Figure S1: *Synechocystis* cultures incubated with methanol over 7 days at concentrations of 0, 16 and 64 mg L^{-1}, corresponding to methanol concentrations present in ^{13}C-PFOS at concentrations of 0, 1 and 4 mg L^{-1} respectively. Cells incubated with 64 mg L^{-1} formed cell clusters.